Unfractionated heparin inhibits live wild-type SARS-CoV-2 cell infectivity at therapeutically relevant concentrations.

Julia A Tree [a*~], Jeremy E Turnbull [be~], Karen R Buttigieg [a], Michael J Elmore [a], Naomi Coombes [a], John Hogwood [c], Courtney J Mycroft-West [d], Marcelo A Lima [d], Mark A Skidmore [d], Richard Karlsson e, Yen-Hsi Chen [e], Yang Zhang [e], Cosma Mirella Spalluto[g], Karl J Staples[g], Edwin A Yates [b], Elaine Gray [ch], Dave Singh [f], Tom Wilkinson [g], Clive P Page [h], Miles W Carroll [ai].

[a] *National Infection Service, Public Health England, Porton Down, Salisbury, Wiltshire SP4 0JG, United Kingdom.*

[b] *Department of Biochemistry and Systems Biology, Institute of Systems, Molecular & Integrative Biology, University of Liverpool, Biosciences Building, Liverpool, L69 7ZB, United Kingdom.*

[c] *Haemostasis Section, Biotherapeutics, National Institute for Biological Standards and Control (NIBSC), Blanche Lane, South Mimms, Hertfordshire, EN6 3QG, United Kingdom.*

[d] *Molecular & Structural Biosciences, School of Life Sciences, Keele University, Newcastle-Under-Lyme, Staffordshire, ST5 5BG, UK*

[e] *Copenhagen Center for Glycomics, Department of Cellular & Molecular Medicine, University of Copenhagen, Copenhagen N 2200, Denmark*

[f] *Medicines Evaluation Unit, University of Manchester, Manchester University Hospital NHS Foundation Trust, Manchester, United Kingdom*

[g] *Department of Respiratory Medicine, University of Southampton, Southampton, United Kingdom.*

[h] *Sackler Institute of Pulmonary Pharmacology, King's College London, London, United Kingdom.*

[i]*Nuffield Department of Medicine, Medawar Building, Oxford University, Oxford, OX1 3SY, United Kingdom.*

~Julia A Tree & Jeremy E Turnbull are joint first authors

*corresponding author

Dr Julia A Tree, National Infection Service, Public Health England, Porton Down, Salisbury, Wiltshire, SP4 0JG, United Kingdom

Email: julia.tree@phe.gov.uk

Telephone: +44 (0) 1980 612100

ACKNOWLEDGEMENTS

This study was funded by Public Health England. We thank Professor Jan Shute (University of Portsmouth) for helpful comments on nebulised heparin. We add thanks to Dr Julian Druce, Doherty Institute, Melbourne, Australia for donating the virus used in this study. We thank Dr Kevin Bewley, Public Health England for designing and optimising the PRNT assay used in this study. We are grateful for receiving MERS convalescent sera from Dr Mark Page and Dr Giada Mattiuzzo, NIBSC, UK. Dave

Singh is supported by the National Institute for Health Research (NIHR) Manchester Biomedical Research Centre (BRC).

CONFLICT OF INTEREST

All authors have no conflicts of interest to declare.

ABSTRACT

Background and Purpose: Currently there are no licensed vaccines and limited antivirals for the treatment of COVID-19. Heparin (delivered systemically) is currently used to treat anticoagulant anomalies in COVID-19 patients. In addition, in the UK, Brazil and Australia, nebulised unfractionated heparin (UFH) is being trialled in COVID-19 patients as a potential treatment. A systematic comparison of the potential antiviral effect of various heparin preparations on live wild-type SARS-CoV-2, *in vitro*, is needed.

Experimental Approach: A range of heparin preparations both UFH (n=4) and low molecular weight heparins (LMWH) (n=3) of porcine or bovine origin were screened for antiviral activity against live SARS-CoV-2 (Australia/VIC01/2020) using a plaque reduction neutralisation assay with Vero E6 cells. Interaction of heparin with spike protein RBD was studied using differential scanning fluorimetry, and the inhibition of RBD binding to human ACE2 protein using ELISA assays was examined.

Key Results: All the UFH preparations had potent antiviral effects, with IC_{50} values ranging between 22-60 μg/ml whereas LMWHs were significantly ($P<0.001$) less inhibitory by ~100-fold (IC_{50} range 4.3–7.8 mg/ml).

Mechanistically we observed that heparin binds and destabilizes the RBD protein, and furthermore we show heparin directly inhibits the binding of RBD to the human ACE2 protein receptor.

Conclusions and Implications: This comparison of clinically relevant heparins shows UFH has significantly stronger SARS-CoV-2 antiviral activity compared to LMWHs. UFH acts to directly inhibit binding of spike protein to the human ACE2 protein receptor. Overall the data strongly support further clinical investigation of UFH as a potential treatment for patients with COVID-19.

What is already known

Systemically administered UFH and LMWH are routinely used in the treatment of COVID-19 as anticoagulants. Evidence suggests UFH has antiviral activity.

What this study adds

A systematic comparison of the antiviral activity of a range of clinically relevant UFH and LMWH, and direct evidence for mechanism of action via inhibition of spike protein interaction with the human ACE2 protein receptor.

What is the clinical significance

UFH has potent antiviral properties at clinically relevant doses and is superior compared to LMWH, justifying the selection of an UFH for investigation as a potential nebulised treatment for patients with COVID-19.

Keywords: COVID-19; SARS-CoV-2; heparin; LMWH; UFH; nebulised

1 INTRODUCTION

Currently there are no licensed vaccines and limited antivirals for the treatment of COVID-19. Repurposing existing clinical drugs with proven safety profiles provides a rapid approach to address this gap in treatment. Throughout the COVID-19 pandemic anticoagulant drugs such as unfractionated heparin (UFH) and low molecular weight heparin (LMWH) delivered systemically, have been widely used across the world as part of standard treatment for patients in intensive care units (ICU). Use of these drugs has been shown to be effective for dealing with coagulopathies seen during the late stage of the disease (Kollias, Kyriakoulis et al., 2020; Tang, Li et al., 2020). Furthermore, heparin exhibits a wide range of anti-inflammatory properties (Mulloy, Hogwood et al., 2016), thus providing an additional rationale of its clinical use to treat the hyperinflammatory response observed in patients with COVID-19.

There is a recent and growing body of evidence suggesting that UFH has antiviral properties against SARS-CoV-2, the causative agent of COVID-19. UFH has been shown to bind to the receptor binding domain (RBD) of the SARS-CoV-2 spike protein, which induces a conformational change (Mycroft-West, Su et al., 2020a) and also inhibits binding of spike protein to cells (Mycroft-West, Su et al., 2020b; Partridge, Green et al., 2020). Additional work with a pseudotyped assay indicated that UFH has a half inhibitory maximal concentrations (IC_{50}) of 0.6 µg/ml (Tandon, Sharp et al., 2020). Recent studies, performed with live SARS-CoV-2 and Vero E6 cells, were limited to one heparin brand (Celsus, USA) and showed SARS-CoV-2 virus was inhibited by 44 - 80% with 6.25 µg - 200 µg/ml of UFH *in vitro* (Mycroft-West, Su et al., 2020b). Conzelmann et al also report that heparin, sourced from the company Sigma-

Aldrich, suppressed viral replication of SARS-CoV-2 in Vero E6 cells by 60% using 125-250 μg/ml and most recently Clausen et al also show a concentration dependent inhibitory effect of UFH across the range of 1-100 μg/ml in Vero E6 cells and they reported a 5-fold reduction in virus infection in primary human bronchial epithelial cells (Clausen, Sandoval et al 2020).

The accurate determination of the amount of heparin (μg/ml) required to inhibit 50% of wild-type, authentic, live SARS-CoV-2 virus has yet to be reported in an in vitro system and a systematic assessment of the antiviral activity of different commercially available heparins, already in clinical use, has yet to be performed. Once determined, though, such an analysis should inform the selection of the most appropriate heparin preparation having the most antiviral activity. The determination of the IC50 of different heparin preparations will also enable a quantitative comparison between different heparin sources eg, bovine and porcine, and heparins with different molecular weights eg. UF and LMWH. Such a systematic analysis should also enable a quantitative comparison with other drugs under investigation as treatments for COVID-19 eg, remdesivir.

Independent from the systemic use of heparin in COVID-19 patients, nebulised heparin has been proposed as a unique and potentially effective treatment for different stages of COVID-19 disease (van Haren, Page et al., 2020). In the UK a clinical trial evaluating the effectiveness of nebulised UFH in hospitalised COVID-19 patients is currently underway (https://accord-trial.org). The strategy underpinning this treatment stems from the positive observations made, based on anticoagulant and anti-inflammatory activity, when running trials of nebulised heparin in patients with acute

lung injury and other respiratory conditions (van Haren, Page et al., 2020). The delivery of an aerosolised antiviral agent directly to the lungs where SARS-CoV-2 virus is known to be present (both upper and lower respiratory tract) (Schaefer, Padera et al., 2020) may help to treat the alveolar coagulopathy that is often a feature of COVID-19, reduce the hyperinflammatory response and prevent patients from developing acute respiratory distress syndrome (ARDS) and pulmonary fibrosis (PF), the major complications of infection with SARS-CoV-2.

Here we report for the first time a systematic assessment of the antiviral activity of a range of heparins (UFH and LMWH) *in vitro* against live wild-type SARS-CoV-2 thereby shedding light on the antiviral potency of a range of different heparin preparations, including the nebulised UFH already undergoing clinical trials in COVID-19 patients. We also report evidence for a direct mechanism of action via inhibition of spike protein RBD to ACE2 protein receptor.

2 METHODS

2.1 Heparin preparations

Clinically used LMWH preparations investigated were: Innohep (tinzaparin sodium, LEO Pharma), Clexane (enoxaparin sodium, Sanofi) and Fragmin (dalteparin sodium, Pfizer), along with a porcine mucosal UFH (heparin sodium, Wockhardt, UK) [currently being investigated by nebulisation in a UK human clinical trial. Further heparin preparations investigated were, a porcine mucosal UFH preparation (Celsus, USA)

and both a bovine lung heparin (Calbiochem) and a bovine mucosal heparin (15/110, NIBSC, UK).

Specific anticoagulant activity for the UFH preparations were measured as described in the United States Pharmacopeia general monograph for assay of heparin (U.S.P.). The molecular weights for the UFH and LMWH samples were measured as previously described (Mulloy & Hogwood, 2015). The specific activity of the clinical LMWHs was taken from the clinical product information (Clexane, 100 IU/mg; Innohep, 100 IU/mg; Fragmin 130 IU/mg).

2.2 Plaque reduction neutralisation assay

SARS-CoV-2 (hCov-19/Australia/VIC01/2020) (Caly, Druce et al., 2020) was generously provided by The Doherty Institute, Melbourne, Australia at P1 and passaged twice in Vero/hSLAM cells [ECACC 04091501]. Whole genome sequencing was performed, on the working stock at Passage 3, using both Nanopore and Illumina as described previously (Lewandowski, Xu et al., 2019) and no significant changes in the viral sequence were observed. Virus titre was determined by a plaque assay on Vero E6 cells [ECACC 85020206]. Cell lines were obtained from the European Collection of Authenticated Cell Cultures (ECACC) PHE, Porton Down, UK. Cell cultures were maintained at 37^{o}C in minimal essential media (MEM) (Life Technologies, California, USA) supplemented with 10% foetal bovine serum (FBS) (Sigma, Dorset, UK) and 25 mM HEPES (Life Technologies).

All heparin preparations were diluted, 5-fold in MEM (Life Technologies) containing 1% (v/v) FBS (Life Technologies), 1x antibiotic/antimycotic (Life Technologies) and 25 mM HEPES buffer (Sigma) (PRNT media) by diluting down in a 96 well plate. Dilutions were made fresh on the day of the assay. SARS-CoV-2 was diluted to a concentration of 933 pfu/mL (70 pfu/75µl) in PRNT media and mixed 50:50 with heparin dilutions, in a 96-well V-bottomed plate. The plate was incubated at 37°C in a humidified box for 1 hour to allow the virus to be exposed to heparin. The neutralised virus was transferred onto the wells of a washed 24-well plate that had been seeded with Vero E6 cells the previous day at 1.5 x 10^5 cells/well. The virus/heparin mixture was left to adsorb for an hour at 37°C, then plaque assay overlay media was applied (MEM containing 1.5% carboxymethylcellulose (Sigma), 4% (v/v) FBS and 25mM HEPES buffer). After incubation at 37ºC in a humidified box, for 5 days, plates were fixed overnight with 20% (v/v) formalin/PBS, washed with tap water and then stained with methyl crystal violet solution (0.2% v/v) (Sigma) and plaques were counted. Heparin dilutions were performed in either triplicate or quadruplicate. Heparin dilutions with cells only were also run in duplicate, to determine if there was any cell cytotoxicity.

An internal positive control for the PRNT assay was run in duplicate using a sample of heat-inactivated human MERS convalescent serum known to neutralise SARS-CoV-2 (National Institute for Biological Standards and Control [NIBSC], UK).

2.3 Recombinant RBD-SD1 expression and purification

Secreted Spike protein RBD-SD1 was transiently produced in suspension HEK293-6E cells. A plasmid encoding RBD-SD1, residues 319−591 of 2019-nCoV S were

cloned upstream of a C-terminal HRV3C protease cleavage site; a monomeric Fc tag and an His8x Tag were a gift from Jason S. McLellan, University of Texas at Austin, USA. Briefly, 100 mL of HEK293-6E cells were seeded at a cell density of 0.5 × 106 cells/ml 24 hr before transfection with polyethyleneimine (PEI). For transfection, 100 µg of the ACE2 plasmid and 300 µg of PEI (1:3 ratio) were incubated for 15 min at room temperature. Transfected cells were cultured for 48 hr and fed with 100 mL fresh media for additional 48 hr before harvest. RBD-SD1 was purified by HiTrap Protein G HP column (GE Healthcare, US) pre-equilibrated in PBS and eluted with 0.1M glycine (pH 2.7). Purity of proteins was evaluated by Coomassie staining of SDS-PAGE gels, and proteins were quantified by BCA Protein Assay Kit (Thermo Scientific).

2.4 Differential scanning fluorimetry

Differential scanning fluorimetry (DSF) was performed employing the hydrophobic dye Sypro orange (1.25 X; Invitrogen) to monitor the thermal denaturation of RBD-SD1 (1 µg/well) alone or in the presence of 200 µg heparin (Celsus or Wockhardt) in PBS pH 7.6 with a total well volume of 40 µL. To ensure that a change in melting temperature was not a result of interactions between Sypro orange and heparin (Celsus or Wockhardt), control wells containing H2O or heparin (Celsus or Wockhardt) without mS1-RBD were also screened. Melt curve experiments were performed in 96-well qPCR plates (AB Biosystems) using an AB biosystems StepOne plus qPCR machine with the TAMRA filter setting enabled. An initial incubation of 2 minutes at 25 °C was set, increasing sequentially by 0.5 °C increments every 30 s up to 90°C. Melt curves were smoothed (9 neighbours, 2nd-order polynomial, Savitxky-Golay) and first differential plots were constructed utilising Prism 8 (GraphPad). The peak of the first

differential plots were used to calculate Tm values using MatLab software (R20018a, MathWorks) and the difference between mean values (n = 3) was calculated using a t-test in Prism 8 (GraphPad).

2.5 ELISA assay for measuring inhibition of RBD-ACE2 binding

3 µg/mL streptavidin (Fisher) in 50 mM sodium carbonate buffer pH 9.6 (50 µL/ well) was incubated for 1 hour at 37 ^{o}C in high binding 96-well plates (Greiner). Plates were blocked with PBS, 0.2% Brij35 (w/v) + 1% casein (w/v) for 1 hour at 37 ^{o}C, after washing thrice with PBS, 0.2% Brij35 (w/v) (PBSB). Plates were washed again with PBSB and then incubated with biotinylated-ACE2 (Sino Biological) in PBSB + 1% (w/v) casein for 1 hour at 37 ^{o}C. mS1-RBD in PBSB + 1% casein (w/v) was pre-incubated separately for 30 minutes at r.t. with or without heparin at distinct concentrations (100 - 0.7 µg/mL), before addition to the pre-washed plates containing immobilised ACE2. Plates were subsequently incubated for 1 hour at 37 $^{\circ}$C and washed with PBSB. Bound mS1-RBD was detected by incubation with 0.5 µg/mL Rabbit-SARS-CoV-2 (2019-nCoV) Spike RBD Antibody (Stratech) in PBSB + 1% (w/v) casein (50 µL/well) for 1 hour at 37 ^{o}C. Plates were washed thrice with PBSB before being incubated for 30 minutes at 37 ^{o}C with horseradish peroxidase-conjugated Donkey anti-Rabbit IgG, diluted 1:1000 (v/v) in PBSB + 1% casein (w/v) (Biolegend). Plates were washed thoroughly with PBSB before being developed with 3,3',5,5'- tetramethylbenzidine prepared according to the manufacturer's instructions (Sigma). After 10 minutes colour development, the reaction was stopped through the addition of 20 µL, 2M HsSO4 and well-absorbances were determined at λ =450 nm using a Tecan Infinate M200 Pro

multi-well plate reader (Tecan Group). Control wells containing no biotinylated ACE2 were employed to ensure binding was specific.

2.6 Statistical analysis

A mid-point probit analysis (written in R programming language for statistical computing and graphics) was used to determine the amount of heparin (µg/ml) required to inhibit SARS-CoV-2 viral plaques by 50% (IC_{50}) compared with the virus only control (n=10). Analysis was conducted in R (R Project, 2019) and the script was based on a source script from Johnson *et al* 2013 (Johnson, Dahlgren et al., 2013) A 2-samplet Student's t-test was used to compare the IC_{50} values of different heparins, this analysis was conducted in R.

3 RESULTS

The characteristics of the different UFH and LMWHs are detailed in Table 1. A concentration dependent relationship between the amount of heparin (µg/ml) and the antiviral activity against SARS-CoV-2 was observed. The data from representative plaque reduction neutralisation assays are plotted for UF heparins (Figure 1) and LMWHs (Figure 2).

3.1 Unfractionated heparin

The two porcine unfractionated heparins obtained from Wockhardt (clinical batch) and Celsus had average IC_{50} values of 41 µg/ml and 22 µg/ml, respectively (Table 1).

However, there was no significant difference ($P > 0.05$) between these two heparins. The bovine mucosa UFH (60 µg/ml) was slightly less potent than porcine UFH (22 & 41 µg/ml) however this was not significantly different ($P > 0.05$). There was no significant difference ($P > 0.05$) between the antiviral activity (IC_{50}) of bovine lung (27 µg/ml) and heparin derived from bovine mucosa (60 µg/ml) (Table 1).

3.2 Low molecular weight heparins

LMWHs varied in activity but were typically ~100-fold lower in antiviral activity compared with UFHs (Table 1, Figure 2). Of the LMWHs, Innohep was the most potent with a IC_{50} value of 4.3 mg/ml. Clexane was the least effective with an inhibitory activity/IC_{50} of 7.8 mg/ml. There was no significant difference ($P > 0.05$) between the antiviral activity of these different LMWHs preparations.

3.3 Comparison of UF and LMW heparins

Since there was no significant difference between the different preparations of UFH the data was grouped (n=14) and the data for the LMWH preparations was grouped (n=10) (as no significant difference was seen between LMWH preparations). When compared, using a 2-sample t-test there was a significant difference ($P < 0.001$) between the IC_{50} values for UF and LMWH, indicating the antiviral activity of UF is significantly greater than LMWH.

3.3 Effect of Molecular Weight

The antiviral activity shown by the different heparins appeared to correlate broadly with their molecular weight. Overall UFHs with the highest molecular weights ranging between 15,650 – 19,100 Da were more potent inhibitors of SARS-CoV-2 than low molecular weight heparins ranging between 4,200 - 6,650 Da (Table 1).

3.4 Mechanisms of action of heparin against SARS-CoV-2 – destabilisation of spike protein RBD and inhibition of RBD binding to human ACE2

Since previous work has indicated interactions of heparin with spike protein RBD we first confirmed a direct interaction of UF heparins with soluble S1 RBD domain (RBD-SD1) expressed in HEK239 cells by exploring their effects on protein thermal stability using differential scanning fluorimetry (DSF). DSF exploits conventional real time PCR machines to monitor the thermal denaturation of a protein through a range of temperatures, in the presence of a hydrophobic fluorescent dye. Upon heating the hydrophobic regions of proteins become exposed upon unfolding, resulting in increased fluorescence. The midpoint of unfolding (Tm) can be determined through the first differential of the resulting melt curve and changes in Tm values in the presence of ligands can be used to determine binding affinity (Nisen, Berglund and Vedadi, 2007). This method has previously been exploited to characterise the structural requirements of heparin for binding to fibroblast growth factors (Uniewicz, Ori et al., 2010). Both Celsus and Wockhardt UF heparin with RBD-SD1 exhibited a significant reduction in the melting temperature (ƛTm) of >4^{o}C (Figure 3A and B; Celsus UF, 4.5^{o}C; Wockhardt UF, 4.2^{o}C). This confirmed their direct interaction with RBD, and furthermore suggests a significant destabilisation of the RBD protein structure which could alter its ability to interact with ACE2 cell receptor.

In order to both validate the human relevance of our data, and also evaluate the potential mechanism by which heparin might inhibit SARS-CoV-2 binding to human cells, we utilized an ELISA assay with surface immobilised recombinant human ACE2 to measure the binding of RBD-SD1. Binding of RBD-SD1 to human ACE2 protein was confirmed by detection with an anti-RBD antibody (Figure 4). A concentration response assay using Celsus UFH demonstrated clear inhibition of binding, with an IC_{50} of ~24 µg/ml (Figure 4). These data are in very close agreement with the heparin inhibition data for live SARS-CoV-2 infectivity of Vero cells (Table 1). Notably, these data support the human relevance of our data on the inhibition of SARS-CoV-2 infection of Vero E6 cells by heparins, and provides strong evidence for a direct mechanism in which heparin destabilises the spike protein RBD and inhibits its binding to the ACE2 protein receptor.

4 DISCUSSION

Some studies have already reported the association between treatment with systemically administered heparin and lower mortality in patients admitted to hospital with COVID-19 (Ayerbe, Risco et al., 2020; Tang, Bai et al., 2020), assumed to be a consequence of the known anticoagulant effect. Coagulopathies have caused major problems in late stage COVID-19 disease (Kollias, Kyriakoulis et al., 2020) and the use of heparin in the treatment of COVID-19 has become part of the standard care for many patients in ICU. However, the dose and type of heparin (UFH or LMWH) delivered either by the sub-cutaneous or intravenous route varies across the world.

Regarding standard systemic usage, the therapeutic range for UFH is typically 0.3 - 0.7 IU/ml (~2 - 4 µg/ml) (Hirsh, Anand et al., 2001), with peak dosing concentrations reaching ~10 - 20 µg/ml. It is reassuring to see that the range of IC_{50} for UFH is 22-60 µg/ml is close to the peak dosing range suggesting that at least partial antiviral effects could be expected in this setting. It is also feasible that heparin could be used in combination with alternative anti-viral agents acting via different mechanisms, in order to gain therapeutic advantage.

In the UK, Brazil and Australia, in addition to systemic heparin use, a novel approach of delivering UFH via nebulisation directly to lungs of COVID-19 patients is undergoing evaluation in a clinical trial by the ACCORD clinical trials platform (https://accord-trial.org/) (van Haren, Page et al, 2020), seeking to gain benefit from the additional known anti-inflammatory activity of heparin, and to provide high local anti-coagulant effects on the alveolar region of patients with severe COVID-19. Nebulisation allows for the targeting of lung tissue directly and therefore impact upon the local hyperinflammatory response and alveolar coagulation resulting from SARS-CoV-2 viral load in the lung. During the UK trial UFH (Wockhardt) will be administered at 25,000 IU (130 mg) every 6 h to patients. The efficiency of nebulising UFH through a high efficiency mesh nebuliser is estimated to be about 20 %, thus the delivered dose to the lung is ~ 26 mg. Assuming the normal human airway surface fluids are in the range 10 - 60 ml (Frohlich, Mercuri et al., 2016), the peak amount of UFH delivered to the lung should be ~400 - 2600 µg/ml, though these values could be lower if diluted by increased fluid volumes as a result of pulmonary oedema. Even allowing for this, these values greatly exceed the IC_{50} of 41 µg/ml reported here for the same batch of Wockhardt UFH as used in the current UK clinical trial. Thus, nebulisation of UFH

should provide strong antiviral effects, in vivo. Importantly, inhaled UFH does not enter the systemic coagulation in any meaningful way so that nebulised UFH can be used safely on top of standard of care involving the systemic use of UFH or LMWH as an anticoagulant.

Previous work has demonstrated that LMWHs also bind to the SARS-CoV-2 (Mycroft-West, Su et al., 2020b). However, in the present study we observed that LMWHs were markedly less potent in live SARS-CoV-2 virus assays (IC_{50} values of 4.3 - 7.8 mg/ml) than UFH. Using the results reported here LMWH would appear unlikely to reach sufficient concentration to achieve significant antiviral activity for either systemic or nebulisation delivery. The typical therapeutic range for LMWH for anticoagulant therapy is ~5 - 8 µg/ml (0.6 - 1 IU/ml). Consistent with our data, the relationship (fold difference, 189-fold) between UFH and enoxaparin (Clexane) seen here was similar to that observed by Tandon et al, 2020 using a pseudotyped lentivirus inhibition assay where 180-fold difference was seen (Tandon, Sharp et al., 2020). In addition, LMWHs were also observed to be less potent than UFH for inhibition of cell binding by spike protein (Partridge, Green et al., 2020). However, an important caveat is that the potency of UFH and LMWHs remains to be determined in a suitable range of human cells relevant to those affected in individuals infected with SARS-CoV-2, perhaps especially from respiratory tract tissues.

The results of the present study also suggest a dependency on molecular weight for different UFH and LMWH preparations. A positive correlation between molecular weight and antiviral activity was noted for the various porcine LMWHs (4,200 - 6,650 Da) and UFH preparations tested which supports the hypothesis that UFH is more

active due to its higher molecular weight (15,650-19,100 Da). Consistent with these live virus data, molecular weight dependency for binding of heparin and heparan sulfate saccharides to spike protein has been observed (Liu, Chopra et al., 2020; Mycroft-West, Su et al., 2020a). In terms of a molecular explanation for this effect, data from molecular modelling has indicated multiple binding sites on RBD for heparin, including some near the RBD-ACE2 interface (Mycroft-West, Su et al, 2020b; Clausen, Sandoval et al, 2020). Based on this data we anticipate that longer heparin chains may be able to bind more efficiently to multiple sites, and also potentially extend beyond RBD protein to interfere directly with ACE2 binding, and this would be consistent with our ELISA data demonstrating inhibition of RBD-ACE2 interaction by heparin.

Recent work has demonstrated that cell surface heparan sulfate is a necessary co-receptor with ACE2 that mediates SARS-CoV-2 virus infection of cells (Clausen, Sandoval et al, 2020; Bermejo-Jambrina, Eder et al 2020). Regarding the underlying mechanisms, we provided additional evidence here for the action of heparin to destabilise the RBD protein structure (Figure 3), and notably the first evidence for the ability of heparin to directly inhibit binding of RBD to its protein receptor human ACE2 (Figure 4). Both these pieces of data are supported by recent preliminary observations using native mass spectrometry (Yang, Du et al, 2020). Thus, there is a clear mechanistic basis supporting the notion of targeting these interactions with heparin and related compounds. It is also notable that binding of RBD to human lung cancer cell lines can be potently inhibited by heparin (Clausen, Sandoval et al, 2020), strongly supporting the view that our data showing inhibition of live SARS-CoV-2 infectivity of

monkey Vero E6 cells, a widely used experimental model, will also be relevant in vivo for inhibiting infection of human cells.

In the present study bovine mucosal UFH (IC50, 60 μg/ml) had a slightly lower antiviral potency compared to porcine UFH (22 & 41 μg/ml), although this difference was not statistically significant ($P > 0.05$). The potent antiviral activity seen for both porcine and bovine heparins, suggests that this property is not species dependent. Bovine UFH may provide an additional source of heparin to use during the coronavirus pandemic. Currently therapeutic UFH available in Europe and US is of porcine mucosal origin; however, owing to supply issues there is now interest, specifically in the US, employing bovine mucosal UFH as an additional source to improve the robustness of supply chains (Hogwood, Mulloy et al., 2017; Keire, Mulloy et al., 2015).

The antiviral (IC_{50}) data for the different UFH and LMWHs display no obvious correlation with anticoagulant activities (IU/mg), indicating that different structure-activity relationships exist for antiviral activity. Importantly, this suggests that further investigation of non-anticoagulant heparins (Cassinelli, Torri et al., 2020; Lindahl & Li, 2020) and heparin mimetics (Guimond, Mycroft-West et al., 2020; Lindahl & Li, 2020) is warranted. Mimetics have significant potential to target similar antiviral mechanisms and could be delivered systemically at higher doses to improve efficacy without potential side effects such as bleeding. This would apply to a broad range of patients, not only those requiring anticoagulation. Moreover, mimetics would also provide a fully synthetic route to bypass limitations of heparin supply.

Here we provide evidence for the first time that various types of commercially available and clinically used UFH preparations exhibit potent antiviral efficacy against live wild-type SARS-CoV-2 in vitro. This activity was seen across different preparations of UFH and was also observed with both porcine and bovine heparins and is supported by data indicating a mechanism of action via inhibition of RBD binding to human ACE2. These data indicate that current clinical use of systemic UFH in the treatment of COVID-19 patients in an ICU setting may provide useful antiviral benefits. Moreover, we predict that the delivery of UFH to the lung (via nebulisation) should provide a strong direct antiviral therapy in addition to other documented beneficial effects of heparins.

REFERENCES

Ayerbe, L., Risco, C., & Ayis, S. (2020). The association between treatment with heparin and survival in patients with Covid-19. *J Thromb Thrombolysis*. doi:10.1007/s11239-020-02162-z

Bermejo-Jambrina, M., Eder, J., Kaptein, T.M., Helgers, L.C., Brouwer, J.M., van Hamme, J.L., …Geijtenbeek, T.B.H. (2020) SARS-CoV-2 Infection and Transmission Depends on Heparan Sulfates and Is Blocked by Low Molecular Weight Heparins. *BioRxiv*, doi.org/10.1101/2020.08.18.255810

Bertini, S., Risi, G., Guerrini, M., Carrick, K., Szajek, A. Y., & Mulloy, B. (2017). Molecular Weights of Bovine and Porcine Heparin Samples: Comparison of Chromatographic Methods and Results of a Collaborative Survey. *Molecules, 22*(7). doi:10.3390/molecules22071214

Caly, L., Druce, J., Roberts, J., Bond, K., Tran, T., Kostecki, R., . . . Catton, M. G. (2020). Isolation and rapid sharing of the 2019 novel coronavirus (SARS-CoV-2) from the first patient diagnosed with COVID-19 in Australia. *Med J Aust, 212*(10), 459-462. doi:10.5694/mja2.50569

Cassinelli, G., Torri, G., & Naggi, A. (2020). Non-Anticoagulant Heparins as Heparanase Inhibitors. *Adv Exp Med Biol, 1221*, 493-522. doi:10.1007/978-3-030-34521-1_20

Clausen, T. M., Sandoval, D. R., Spliid, C. B., Pihl, J., Painter, C. D., Thacker, B. E., …..Esko, J. D. (2020) SARS-CoV-2 Infection Depends on Cellular Heparan Sulfate and ACE2. Cell, doi.org/10.1016/j.cell.2020.09.033.

Conzelmann, C., Müller, J. A., Perkhofer, L., Sparrer, K. M. J., Zelikin, A. N. Münch,J., Kleger, A. (2020) Inhaled and systemic heparin as a repurposed direct antiviral drug for prevention and treatment of COVID-19. Clinical Medicine 20. doi: 10.7861/clinmed.2020-0351

Frohlich, E., Mercuri, A., Wu, S., & Salar-Behzadi, S. (2016). Measurements of Deposition, Lung Surface Area and Lung Fluid for Simulation of Inhaled Compounds. *Front Pharmacol, 7*, 181. doi:10.3389/fphar.2016.00181

Guimond, S., Mycroft-West, C., Gandhi, N., Tree, J., Buttigieg, K., Coombes, N., . . . Turnbull, J. (2020). Pixatimod (PG545), a clinical-stage heparan sulfate mimetic, is a potent inhibitor of the SARS-CoV-2 virus. *bioRxiv. 2020.06.24.169334*.

Hirsh, J., Anand, S. S., Halperin, J. L., and Fuster, V. (2001). Guide to anticoagulant therapy: Heparin: a statement for healthcare professionals from the American Heart Association. *Circulation, 103*(24), 2994-3018.

Hogwood, J., Mulloy, B., & Gray, E. (2017). Precipitation and Neutralization of Heparin from Different Sources by Protamine Sulfate. *Pharmaceuticals (Basel), 10*(3). doi:10.3390/ph10030059

Johnson, R. M., Dahlgren, L., Siegfried, B. D., & Ellis, M. D. (2013). Acaricide, fungicide and drug interactions in honey bees (Apis mellifera). *PLoS One, 8*(1), e54092. doi:10.1371/journal.pone.0054092

Katarzna. A. U., Orio. A., Xu. R., Ahmed. Y., Wilkinson. M., Fernig. G. D and Yates. A. E. (2010). Differential Scanning Fluorimetry Measurements of Protein Stability Changes upon Binding to Glycosaminoglycans: A Screening Test for Binding Specificity. Anal. Chem. 82(9), 3796-3802

Keire, D. A., Mulloy, B., Chase, C., Al-Hakim, A., Cairatti, D., Gray, E., . . . Soares, M. (2015). Diversifying the global heparin supply chain reintroduction of bovine heparin in the United States? *Pharmaceutical Technology 39*, 2-8.

Kollias, A., Kyriakoulis, K. G., Dimakakos, E., Poulakou, G., Stergiou, G. S., & Syrigos, K. (2020). Thromboembolic risk and anticoagulant therapy in COVID-19 patients: emerging evidence and call for action. *Br J Haematol, 189*(5), 846-847. doi:10.1111/bjh.16727

Lewandowski, K., Xu, Y., Pullan, S. T., Lumley, S. F., Foster, D., Sanderson, N., . . . Matthews, P. C. (2019). Metagenomic Nanopore Sequencing of Influenza Virus Direct from Clinical Respiratory Samples. *J Clin Microbiol, 58*(1). doi:10.1128/JCM.00963-19

Lindahl, U., & Li, J. P. (2020). Heparin - an old drug with multiple potential targets in Covid-19 therapy. *J Thromb Haemost*. doi:10.1111/jth.14898

Liu, L., Chopra, P., Li, X., Wolfert, M. A., Tompkins, S. M., & Boons, G.-J. (2020). SARS-CoV-2 spike protein binds heparan sulfate in a length- and sequence-

dependent manner. *bioRxiv* 2020.2005.2010.087288. doi:10.1101/2020.05.10.087288

Mulloy, B., & Hogwood, J. (2015). Chromatographic molecular weight measurements for heparin, its fragments and fractions, and other glycosaminoglycans. *Methods Mol Biol, 1229*, 105-118. doi:10.1007/978-1-4939-1714-3_11

Mulloy, B., Hogwood, J., Gray, E., Lever, R., & Page, C. P. (2016). Pharmacology of Heparin and Related Drugs. *Pharmacol Rev, 68*(1), 76-141. doi:10.1124/pr.115.011247

Mycroft-West, C., Su, D., Elli, S., Li, Y., Guimond, S., Miller, G., . . . Skidmore, M. (2020a). The 2019 coronavirus (SARS-CoV-2) surface protein (Spike) S1 Receptor Binding Domain undergoes conformational change upon heparin binding. *bioRxiv* 2020.2002.2029.971093. doi:10.1101/2020.02.29.971093

Mycroft-West, C. J., Su, D., Pagani, I., Rudd, T. R., Elli, S., Guimond, S. E., . . . Skidmore, M. A. (2020b). Heparin inhibits cellular invasion by SARS-CoV-2: structural dependence of the interaction of the surface protein (spike) S1 receptor binding domain with heparin. J *bioRxiv* 2020.2004.2028.066761. doi:10.1101/2020.04.28.066761

Niesen. H. F., Berglund. H and Vedadi. M. (2007). The use of differential scanning flurimetry to detect ligand interactions that promote protein stability. *Nature protocols.* 2(9): 2212. doi:10.1038/nprot.2007.321

Partridge, L. J., Green, L. R., & Monk, P. N. (2020). Unfractionated heparin potently inhibits the binding of SARS-CoV-2 spike protein to a human cell line. bioRxiv 2020.2005.2021.107870. doi:10.1101/2020.05.21.107870

R Project. (2019). R: A language and environment for statistical computing. R Foundation for Statistical Computing, Vienna, Austria. https://www.R-project.org/.

Schaefer, I. M., Padera, R. F., Solomon, I. H., Kanjilal, S., Hammer, M. M., Hornick, J. L., & Sholl, L. M. (2020). In situ detection of SARS-CoV-2 in lungs and airways of patients with COVID-19. *Mod Pathol*. doi:10.1038/s41379-020-0595-z

Tandon, R., Sharp, J. S., Zhang, F., Pomin, V. H., Ashpole, N. M., Mitra, D., . . . Linhardt, R. J. (2020). Effective Inhibition of SARS-CoV-2 Entry by Heparin and Enoxaparin Derivatives. *bioRxiv* 2020.2006.2008.140236. doi:10.1101/2020.06.08.140236

Tang, N., Bai, H., Chen, X., Gong, J., Li, D., & Sun, Z. (2020). Anticoagulant treatment is associated with decreased mortality in severe coronavirus disease 2019 patients with coagulopathy. *J Thromb Haemost, 18*(5), 1094-1099. doi:10.1111/jth.14817

Tang, N., Li, D., Wang, X., & Sun, Z. (2020). Abnormal coagulation parameters are associated with poor prognosis in patients with novel coronavirus pneumonia. *J Thromb Haemost, 18*(4), 844-847. doi:10.1111/jth.14768.

Uniewicz, K. A., Ori, A., Xu, R., Ahmed, Y., Wilkinson, M. C., Fernig, D. G., Yates, E. A. (2010) Differential scanning fluorimetry measurement of protein stability changes upon binding to glycosaminoglycans: a screening test for binding specificity. *Anal. Chem.* May 1;82(9):3796-802. doi: 10.1021/ac100188x. PMID: 20353159

U.S.P. United States Pharmacopeia. https://www.usp.org/, *General Chapter 208*.

van Haren, F., Page, C. P., Laffey, M. D., Artigas, A., Camprubi-Rimblas, M., Nunes, Q., . . . Dixon, B. (2020). Nebulised heparin as a treatment for COVID-19: scientific rationale and a global call for randomised evidence. *Critical Care, in press*.

Yang, Y., Du, Y., Kaltashov. I. A. (2020). The utility of native MS for understanding the mechanism of action of repurposed therapeutics in COVID-19: heparin as disruptor of the SARS-CoV-2 interaction with its host cell receptor. *bioRxiv,* doi.org/10.1101/2020.06.09.142794

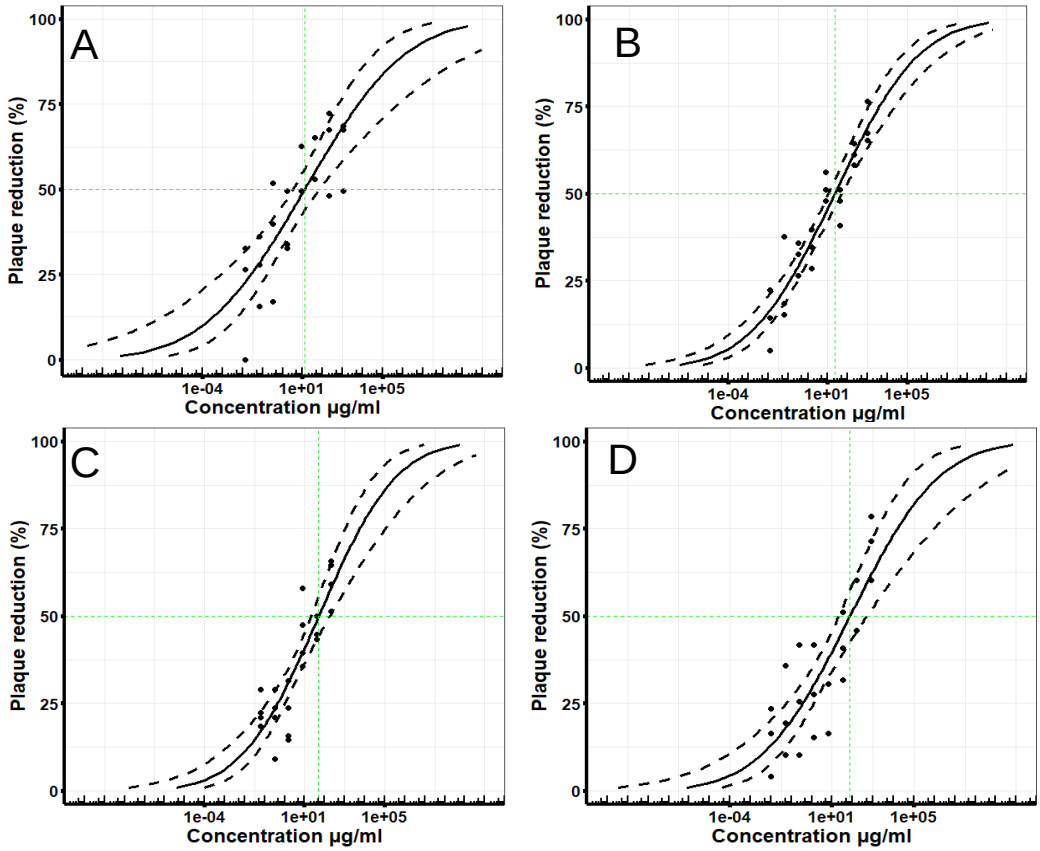

Figure 1: Unfractionated heparins inhibit SARS-CoV-2 infectivity in Vero E6 cells. The % viral plaque reduction caused by increasing concentrations of different unfractionated heparin (UFH) preparations when incubated with live wild-type SARS-CoV-2 *in vitro* with Vero E6 cells. Mid-point probit curves are plotted with 95 % confidence intervals (dashed lines): A) Workhardt UFH (clinical batch), B) Celsus UFH, C) Bovine UFH (lung), D) Bovine UFH (mucosa). There was no significant difference ($P > 0.05$) between the different UFH heparin preparations.

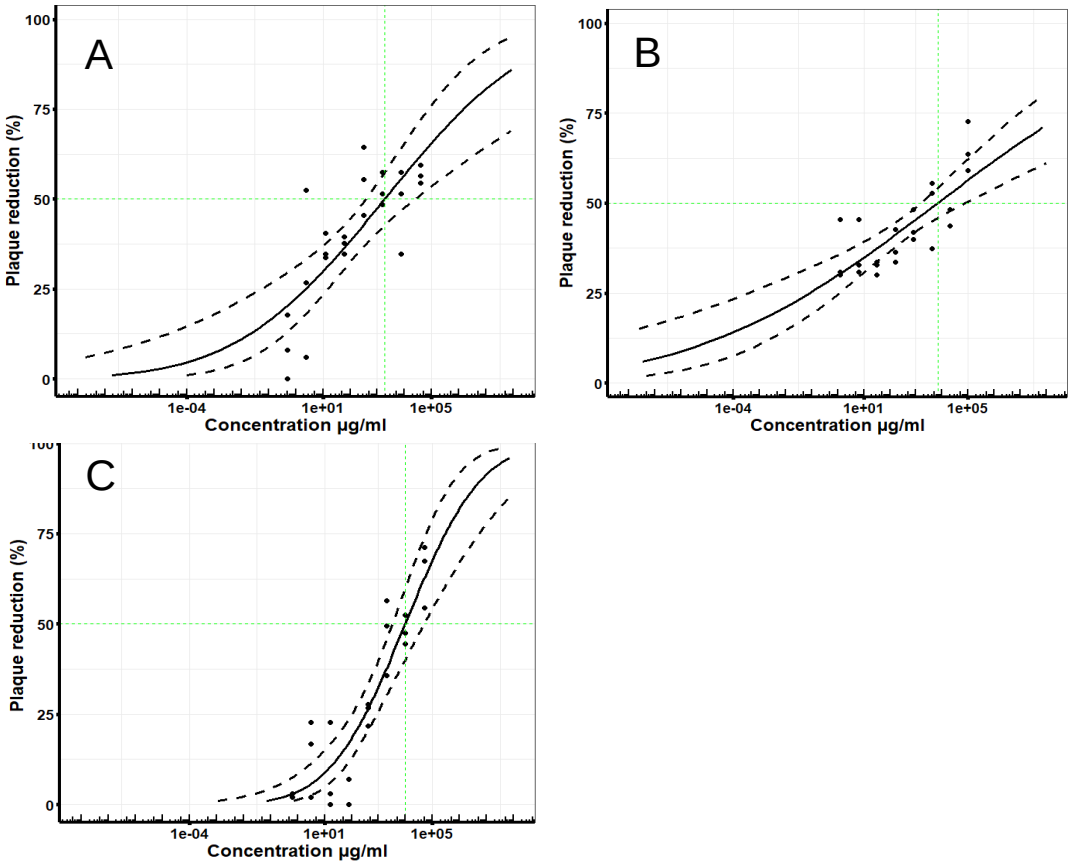

Figure 2: Low molecular weight heparins inhibit SARS-CoV-2 infectivity in Vero E6 cells The % viral plaque reduction caused by increasing concentrations of different low molecular weight heparin (LMWH) preparations when incubated with live wild-type SARS-CoV-2 *in vitro* with Vero E6 cells. Mid-point probit curves are plotted with 95 % confidence intervals (dashed lines): A) Innohep LMWH, B) Fragmin LMWH and C) Clexane LMWH. There was no significant difference ($P > 0.05$) between the different LMWH heparin preparations.

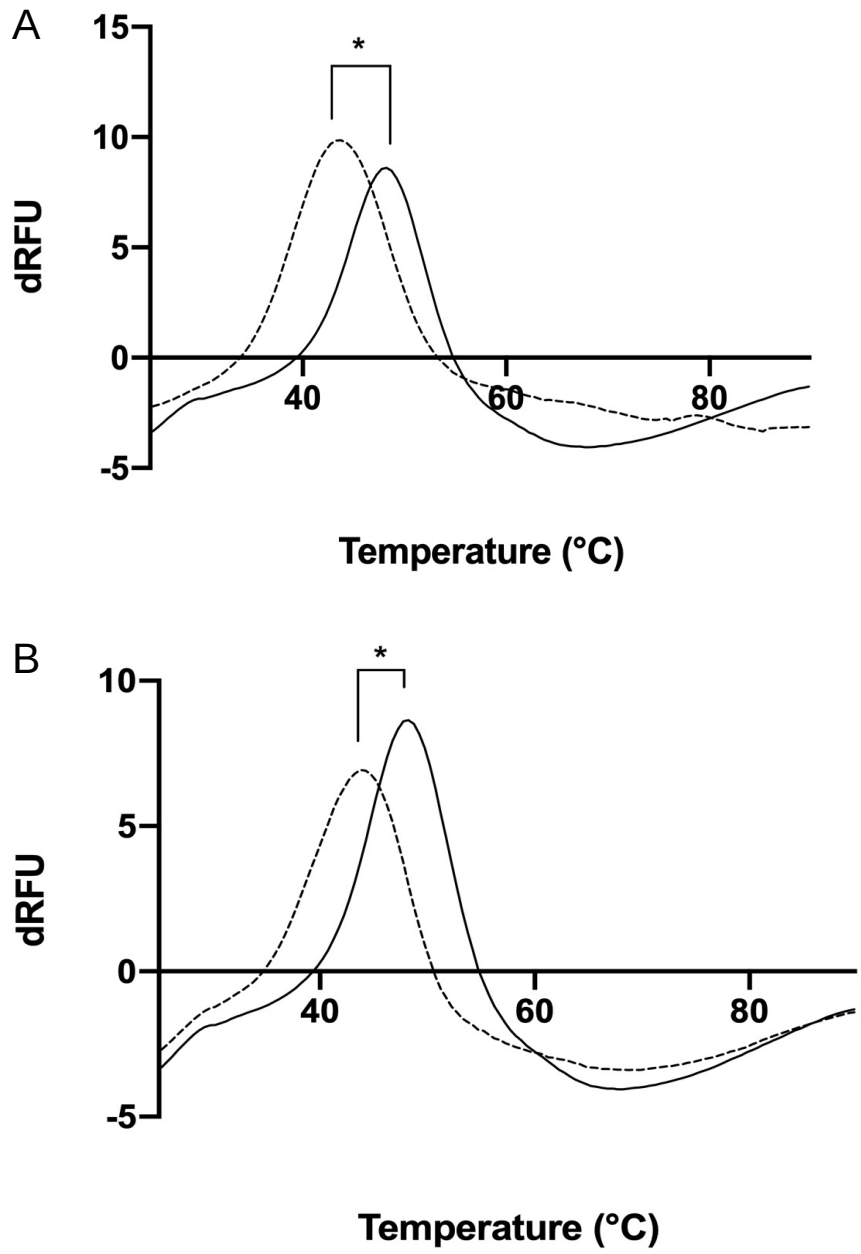

Figure 3: Unfractionated heparins interact directly with spike protein RBD domain. Differential scanning fluorimetry was employed to measure the thermal stability curve for recombinant RBD in the asbsence of presence of UF heparin**.** First differential of the thermal stability of 1 µg RBD alone (solid line) or with 200 µg UF heparin (A, Celsus UF, dashed line; B, Wockhardt UF, dashed line). *Significant difference between the T_m value of RBD (48.3 ° C ± 0; n =3) compared to RBD + Celsus UF (43.8° C ± 1; n = 3), t(2) = 7.8, p= 0.016. ΔT_m = 4.5 ° C; or RBD + Wockhardt UF (44° C ± 0.6; n = 3), t(2) = 12.5, p= 0.0063 ΔT_m = 4.2 ° C.

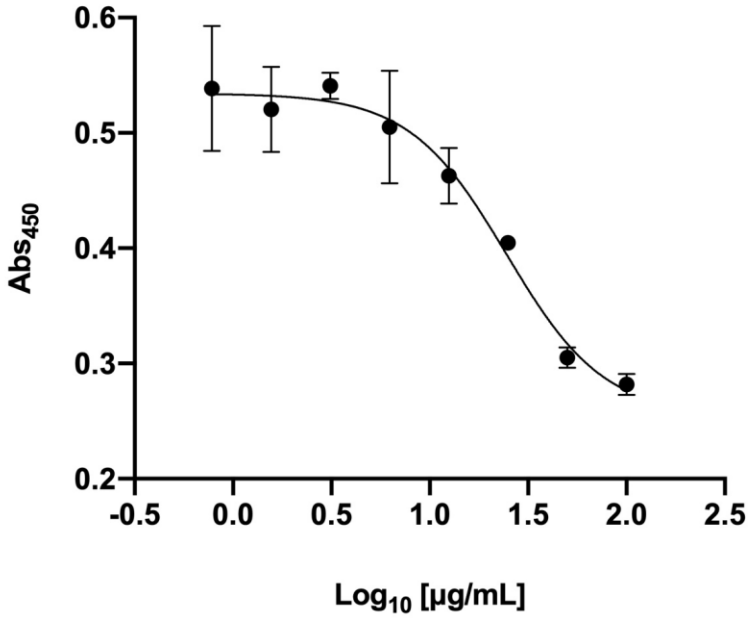

Figure 4: UF heparin directly inhibits binding of spike protein RBD to ACE2 protein receptor. Biotinylated ACE2 was captured onto a high binding microplate coated with streptavidin prior to the addition of RBD pre-incubated with or without varying concentrations of Celsus UF heparin (IC_{50} = 24.6 µg/mL). Detection of bound RBD was achieved with an anti-RBD antibody.

Table 1. Properties of different heparin preparations and their average mid-point probit IC_{50} values, from 3-4 independent experiments

Product	Brand	Origin	Weight Average Molecular weight Da ± 1 SD[a]	Specific Anticoagulant Activity IU/mg (95% Confidence Interval)	Average Probit mid-point (IC_{50}) µg/ml ± 1 SE	Number of independent experiments
Unfractionated heparins						
Heparin sodium	Wockhardt (Clinical Batch[b])	Porcine mucosa	16,300 ± 100	192 (187 – 197)	41 ± 17	4
Heparin sodium	Celsus	Porcine mucosa	15,650 ± 550	192 (186 – 198)	22 ± 5	4
Heparin sodium	Calbiochem	Bovine lung	15,950 ± 550	108 (104 – 112)	27 ± 12	3
Heparin sodium	NIBSC	Bovine mucosa	19,100 ± 200	146 (142 – 152)	60 ± 20	3
Low molecular weight heparins						
Tinzaparin sodium	Innohep	Porcine mucosa	6,650 ± 100	100[c]	4,288 ± 1,294	3
Dalteparin sodium	Fragmin	Porcine mucosa	6,110 ± 50	130[c]	4,640 ± 1,126	4
Enoxaparin sodium	Clexane	Porcine mucosa	4,200 ± 250	100[c]	7,749 ± 988	3

[a] Rounded to the nearest 50 Da, n=2 independent measurements.
[b] This is the same batch of Wockhardt heparin used to treat patients with COVID-19, UK.
[c]These values are based on specific activities quoted by the manufacturers.